UNLIMITED DISTRIBUTION

125721

National Defence
Research and Development Branch

Défense nationale
Bureau de recherche et développement

TECHNICAL MEMORANDUM 92/216
June 1992

AN END-CAPPED CYLINDRICAL HYDROPHONE FOR UNDERWATER SOUND DETECTION

D.F. Jones - S.E. Prasad - S.R. Kavanaugh

Defence Research Establishment Atlantic

Centre de Recherches pour la Défense Atlantique

Canada

DEFENCE RESEARCH ESTABLISHMENT ATLANTIC

9 GROVE STREET
P.O. BOX 1012
DARTMOUTH, N.S.
B2Y 3Z7

TELEPHONE
(902) 426-3100

CENTRE DE RECHERCHES POUR LA DÉFENSE ATLANTIQUE

9 GROVE STREET
C.P. 1012
DARTMOUTH, N.É.
B2Y 3Z7

UNLIMITED DISTRIBUTION

National Defence
Research and Development Branch

Défense nationale
Bureau de recherche et développement

AN END-CAPPED CYLINDRICAL HYDROPHONE FOR UNDERWATER SOUND DETECTION

D.F. Jones - S.E. Prasad - S.R. Kavanaugh

June 1992

Approved by C.W. Bright
Director / Sonar Division

Distribution Approved by C.W. Bright

C W Bright

Director / Sonar Division

TECHNICAL MEMORANDUM 92/216

Defence Research Establishment Atlantic

Centre de Recherches pour la Défense Atlantique

Canada

Abstract

A small end-capped cylindrical hydrophone has been designed and built for use as a low cost, general purpose hydrophone. In the frequency range 15 Hz to 5 kHz, the measured free-field voltage sensitivity of the hydrophone is -195 dB *re* 1 V/μPa, which agrees with the theoretical sensitivity for capped piezoelectric ceramic tubes. In addition, three resonance frequencies below 45 kHz have been measured and identified with circumferential, longitudinal, and flexural modes of vibration.

Résumé

Un petit hydrophone cylindrique à bouchon d'extrémité a été conçu et fabriqué à titre d'hydrophone peu coûteux d'usage général. Dans la plage de fréquences de 15 Hz à 5 kHz, la mesure de sensibilité en tension en champ libre de l'hydrophone est -195 dB re 1 V/μPa, ce qui correspond à la sensibilité théorique pour les tubes à céramiques piézoélectriques à bouchon. De plus, on a mesuré trois fréquences de résonance au-dessous de 45 kHz et on les a identifiées aux modes de vibration sur la circonférence, sur l'axe longitudinal et de flexion.

Contents

List of Symbols

a	inside radius of ceramic cylinder
$\bar{a}$	mean radius of ceramic cylinder
b	outside radius of ceramic cylinder and end caps
B	measured susceptance of the hydrophone
C	total capacitance of four ceramic cylinders in parallel
C_1	capacitance between the electrodes of one ceramic cylinder
C_k	total parasitic capacitance
D	diameter of the hydrophone assembly
d_{31}	piezoelectric charge constant
e	mathematical constant 2.71828...
f	frequency
f_c	circumferential resonance frequency
f_f	flexural resonance frequency
f_f^+	upper bound on the flexural resonance frequency
f_f^-	lower bound on the flexural resonance frequency
f_ℓ	longitudinal resonance frequency
f_ℓ^+	upper bound on the longitudinal resonance frequency
f_ℓ^-	lower bound on the longitudinal resonance frequency
f_r	unloaded ring resonance frequency
g_{31}	piezoelectric voltage constant
g_{33}	piezoelectric voltage constant
k	wavenumber
k_{33}^{T}	free, relative dielectric constant
ℓ	length of ceramic cylinder
L	effective length of the hydrophone assembly
M	free-field voltage sensitivity of ceramic cylinder in decibels
M_k	end-of-cable free-field voltage sensitivity in decibels
n	longitudinal nodal number $1, 3, 5, \ldots$
P_0	external acoustic pressure
s_{11}^{D}	elastic compliance at constant charge density
s_{11}^{E}	elastic compliance at constant electric field
s_{12}^{E}	elastic compliance at constant electric field
s_b	effective elastic compliance
V	open-circuit voltage of the ceramic cylinder
(V/P_0)	free-field voltage sensitivity of ceramic cylinder in V/Pa
$(V/P_0)_k$	end-of-cable free-field voltage sensitivity in V/Pa
α	defined as the ratio a/b
β	defined function of ζ and ξ
δx	error in quantity x
ϵ_0	permittivity of free space 8.85×10^{-12} F/m

ζ	defined function of σ_{12}^{E}
ξ	defined function of $\bar{a}$ and ℓ
π	mathematical constant 3.1415...
ρ	mass density of ceramic cylinder
σ_{12}^{E}	Poisson's ratio at constant electric field

1 Introduction

High sensitivity and low electrical impedance are desirable qualities of wideband hydrophones [1, 2]. Radially-poled piezoelectric ceramic cylinders with end caps possess these characteristics, accounting for their wide spread use in underwater sensor applications. The present cylindrical hydrophone, designated BM024, was developed by B.M. Hi-Tech Inc. to meet the need for a low cost hydrophone for general underwater acoustics work.

A brief description of the hydrophone design is given in Section (2). In-water electroacoustic calibration measurements on the BM024 hydrophone are presented in Section (3). The measurements include free-field voltage sensitivity, electrical conductance and susceptance, and directional response patterns. A detailed theoretical calculation of the sensitivity is found in Sections (4.1) and (4.2). In-air admittance measurements are used to locate all resonances with frequencies lower than the resonance frequency of the circumferential mode. These measurements, along with theoretical predictions for the resonance frequencies, are found in Section (4.3). Finally, the expressions required to evalulate the errors for the various calculated quantities in this paper, are relegated to Appendices A and B.

All of the measurements on the BM024 hydrophone were performed at the acoustic calibration facility of the Defence Research Establishment Atlantic (DREA).

2 Description of the Hydrophone Design

The hydrophone assembly, shown in Fig. 1, consists of four radially-poled cylindrical piezoelectric ceramic elements. The electrodes, on the inside and outside curved surfaces, are connected electrically in parallel. The elements are made of BM500 Navy Type II lead zirconate titanate ceramic, and have an outside diameter of 25.4 mm (1 in), an inside diameter of 19.1 mm (0.75 in), and a length of 12.7 mm (0.5 in). Small ceramic washers isolate the elements from each other, physically and electrically. The washers are made from unpoled Navy Type II ceramic and are 0.5 mm thick.

A brass end cap is fitted to each end of the assembly, and the pressure on the end caps is adjusted using a tension bolt. The end caps provide a tight fit and ensure the integrity of the air gap inside the ceramic elements. The element assembly is then attached to the upper housing and a 3.9 meter coaxial cable. A polyurethane boot is cast, entirely enclosing the element assembly. The boot provides protection for the ceramic elements and electrical contacts, and serves as the acoustic coupling medium between the active elements and the water. The boot also provides stable performance over extended periods of submergence in the harsh ocean environment.

The useful frequency bandwidth for capped cylindrical elements usually depends on the largest dimension of the cylinder and the properties of the end caps [3]. For a single element, the sensitivity is constant for frequencies up to the circumferential resonance, which is determined by the cylinder's mean radius. However, the effective length of the BM024 hydrophone assembly, which includes the four active elements plus passive components such as washers and end caps, constitutes the largest dimension and gives rise to a longitudinal resonance frequency that lies below the circumferential resonance. Furthermore, the stacked configuration of the ceramic elements could permit low-frequency flexural modes, the lowest

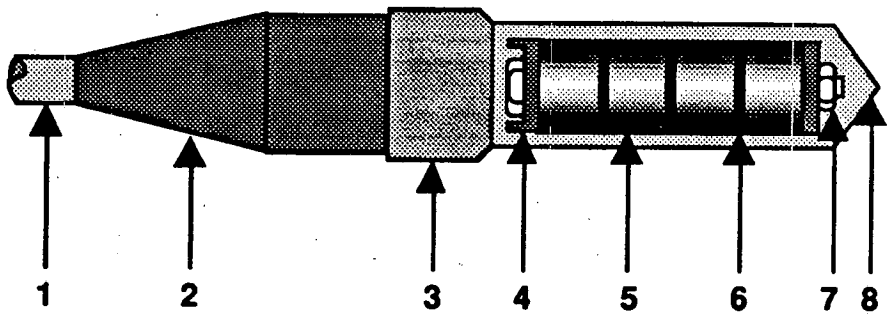

Figure 1: Schematic of a BM024 cylindrical hydrophone manufactured by B.M. Hi-Tech Division of Sensor Technology Limited.

ocurring below the longitudinal mode just mentioned. In any case, one of these modes limits the useful bandwidth at the high frequency end.

The sensitivity is reduced at the low frequency end because the end caps vibrate in a flexure mode. The resonance frequency associated with the flexure mode depends on the elastic modulus and mass density of the end cap material. Flexure in the end caps is more prevalent in hydrophones that consist of several closely stacked cylindrical elements (the present design), than in single element hydrophones, due to inter-element coupling.

3 Electroacoustic Measurements

A BM024 hydrophone was calibrated in the DREA anechoic tank facility. The frequency range investigated was 15 Hz to 10 kHz. The hydrophone was placed at a depth of 1.83 m (6 ft) in fresh water and the water temperature was 20°C. The measurements included the free-field voltage sensitivity, electrical conductance and susceptance, and directional response patterns.

3.1 Free-Field Voltage Sensitivity

The free-field voltage sensitivity of the BM024 hydrophone, measured at the end of a 3.9 m coaxial cable, is shown in Fig. 2. The useful bandwidth is limited to frequencies below 5 kHz due to the presence of a resonance at 7.5 kHz. The sensitivity below 5 kHz is -195 ± 1 dB *re* 1 V/μPa, the error being typical of underwater calibration measurements [4, 5].

Below 50 Hz, we observe an apparent improvement in sensitivity. This slight rise is attributed to a change in tank background noise from the time at which the standard hydrophone was measured to the time at which the BM024 hydrophone was measured. This is a limitation of low frequency calibrations in this facility.

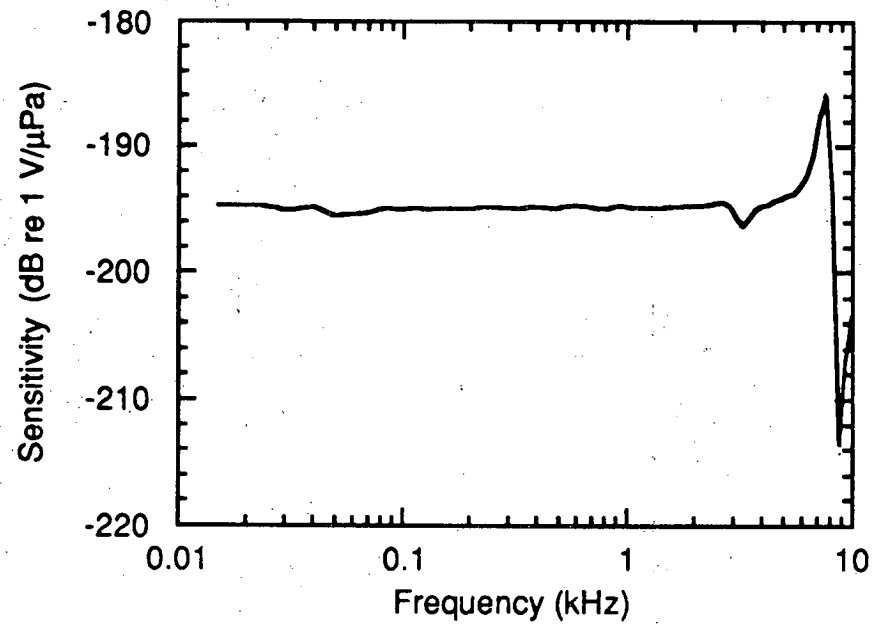

Figure 2: The end-of-cable, free-field, open-circuit voltage sensitivity of the BM024 hydrophone. The frequency ranges from 15 Hz to 10 kHz.

A perturbation due to a spurious resonance appears at 3.2 kHz. Although the 1.5 dB magnitude of the perturbation lies within the ± 1 dB error stated above, the size of the perturbation can vary, depending on the orientation of the hydrophone relative to the calibration source. The perturbation, as a function of angle about the longitudinal axis of the hydrophone, is shown in Fig. 3. The hydrophone was positioned vertically in the water and rotated by intervals of 60°. The source was located in the hydrophone mid-plane (i.e. the plane orthogonal to the longitudinal axis and passing through the center of the hydrophone). The variation in the size of the perturbation is evident. For example, the magnitude of the perturbation, with the source located at 60°, is 1.7 dB, but only 0.8 dB with the source located at 300°.

3.2 Electrical Admittance

The end-of-cable electrical conductance and susceptance, of the BM024 hydrophone, are shown in Fig. 4. The resonance frequency at 7.5 kHz is clearly visible and well behaved. The spurious resonance at 3.2 kHz, alluded to in the previous section, is just visible in the conductance curve, but has a conductance value that is an order of magnitude smaller than that of the 7.5 kHz peak. The value of susceptance at 2 kHz is 236 ± 5 μS, a number that will be used in Section (4.2) to calculate the end-of-cable capacitance of the hydrophone. At the same frequency, the conductance is 5.6 ± 0.1 μS, and therefore, the magnitude of the electrical impedance is 4240 ± 90 Ω.

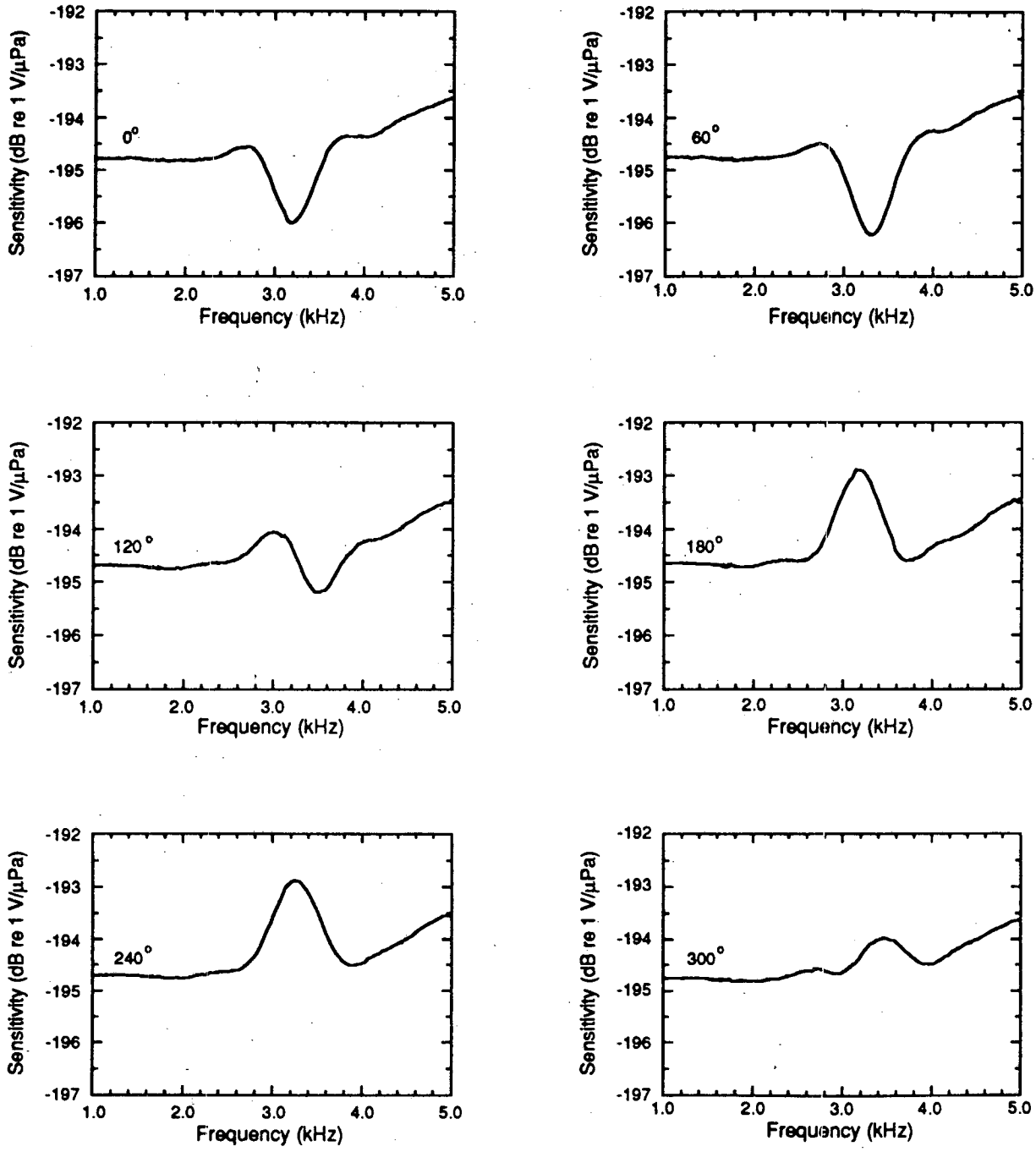

Figure 3: The sensitivity of the BM024 hydrophone as a function of the angle to the source, for the frequency range 1 to 5 kHz.

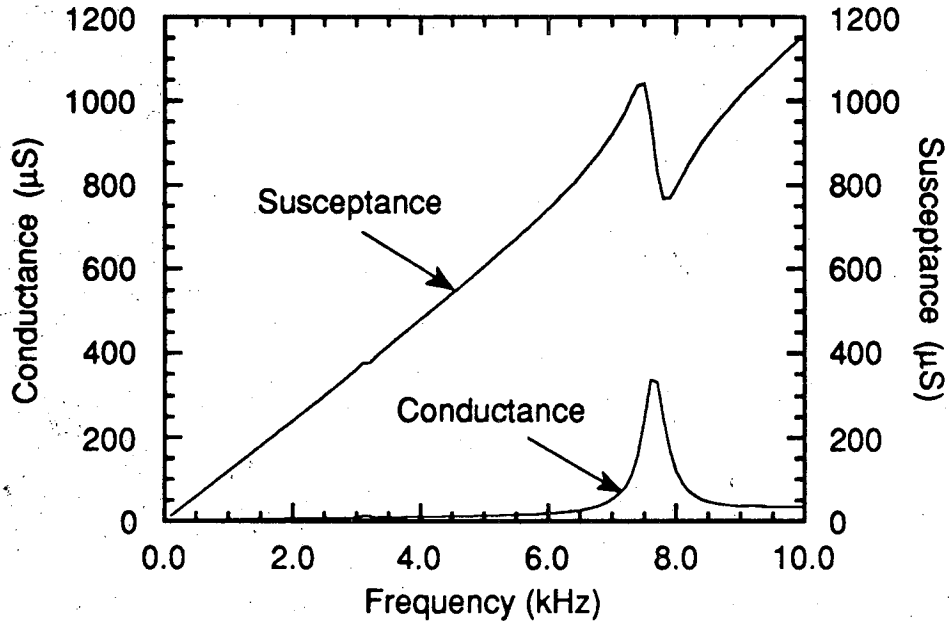

Figure 4: In-water electrical admittance of the BM024 hydrophone, measured at the end of a 3.9 m cable.

3.3 Directional Response

The directivity patterns for the frequencies 2.0, 3.2, 5.0, and 7.5 kHz, are plotted in Figs. 5 and 6. Both the horizontal (XY) plane, i.e. the plane normal to the longitudinal axis of the hydrophone, and the vertical (XZ) plane, are shown.

The XY plots deviate from omnidirectionality by less than ± 1 dB for frequencies below 7.5 kHz, except at the spurious resonance frequency of 3.2 kHz, where the level at 60° is 3.5 dB down from the level at 240°. Of course this is consistent with the corresponding sensitivity plots in Fig. 3.

Below 2 kHz the directivity in the XZ plane is omnidirectional. At 3.2 kHz the level at 0° in the XZ-plane is 1.5 dB down from the level at 180°. At 5 kHz, the level at 90° is 3.5 dB down from the level at 0°. Finally, at the 7.5 kHz resonance frequency, the level at 90° is 4 dB down from the level at 270°. The asymmetry in the XZ pattern at 7.5 kHz, is a direct result of the design differences between the two ends of the hydrophone.

4 Theoretical Calculations

The free-field voltage sensitivity in the frequency band of interest is evaluated for the BM024 cylindrical hydrophone. A correction is included to account for parasitic capacitances in the cable and hydrophone assembly. In addition, all resonance frequencies below 50 kHz are measured in air and compared to theory.

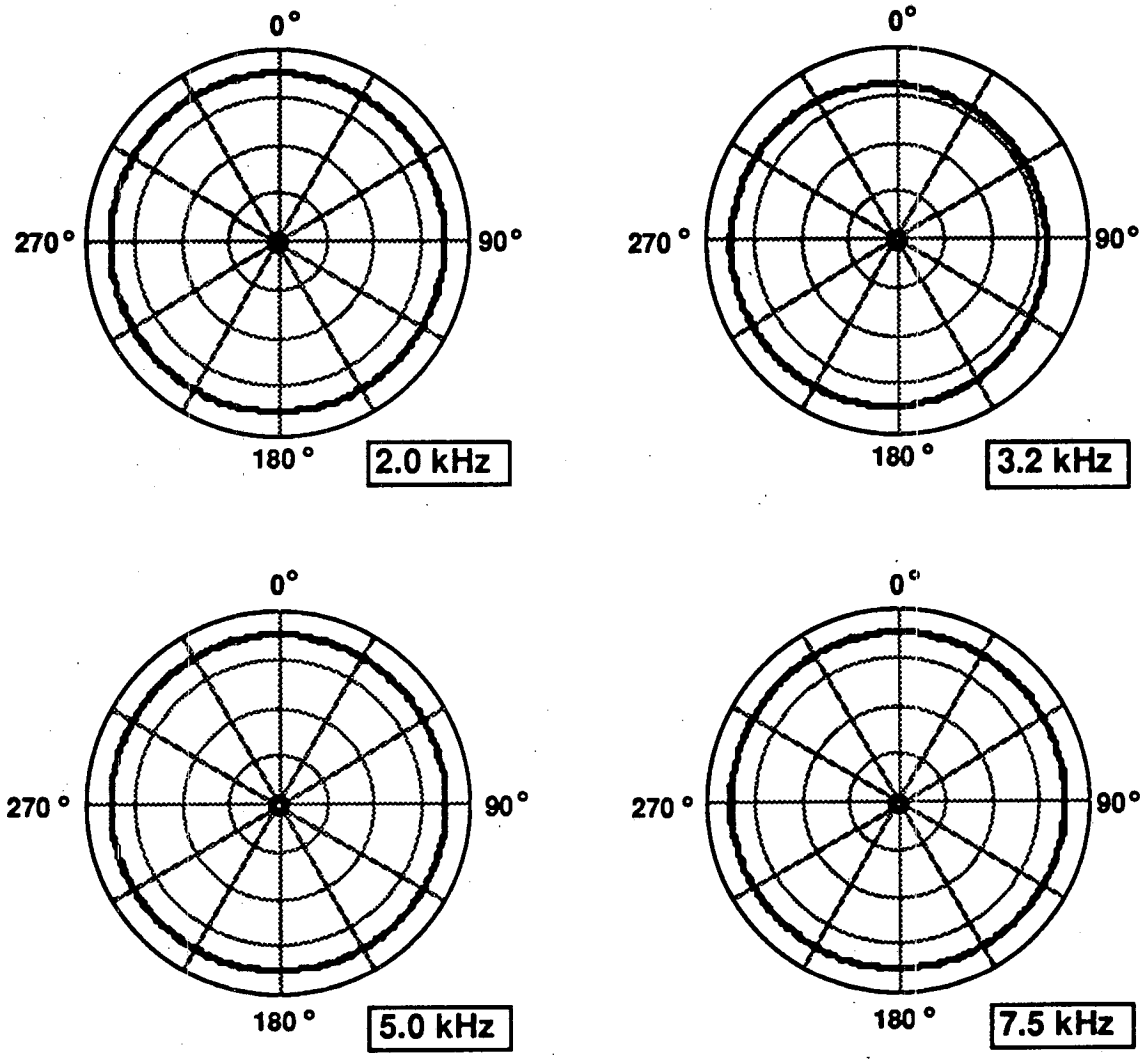

Figure 5: Directivity patterns of the BM024 hydrophone in the horizontal (XY) plane. The scale, from the center to the circumference of the grid in each pattern, is 40 dB.

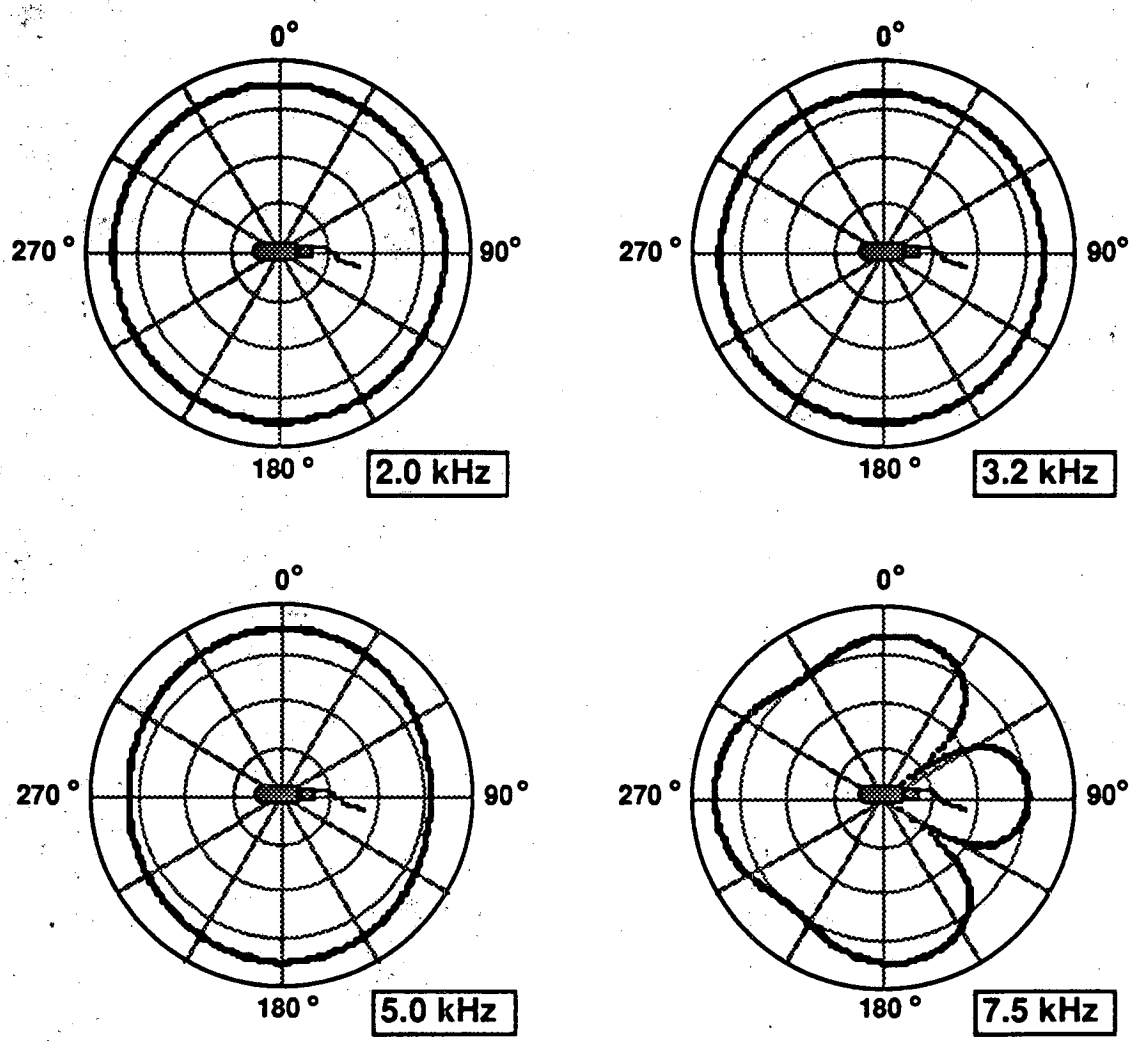

Figure 6: Directivity patterns of the BM024 hydrophone in the vertical (XZ) plane. The scale, from the center to the circumference of the grid in each pattern, is 40 dB.

4.1 Sensitivity of a Cylinder

The sensitivity of a radially-poled, ceramic cylinder with end caps, subjected to a uniform acoustic pressure P_0, has been derived by Langevin [6]. The key assumptions and boundary conditions in the derivation are: (i) the sensitivity corresponds to frequencies well below the first resonance frequency of the cylinder; (ii) the dimensions of the cylinder are small compared to the wavelength; (iii) the inside surface of the cylinder is entirely shielded from the external acoustic pressure, i.e. P_0 vanishes on this surface; (iv) the outside lateral surface is exposed to the external pressure P_0; and (v) the top and bottom annular surfaces are exposed to the magnified pressure $b^2 P_0/(b^2 - a^2)$, the magnification factor being the ratio of the end-cap area to the annular cross-sectional area of the cylinder. Here, a is the inside radius of the ceramic cylinder, and b is the outside radius of both the cylinder and the solid end-caps. The sensitivity is

$$\left(\frac{V}{P_0}\right) = -\left(\frac{b}{1+\alpha}\right)\left[(1-\alpha)g_{33} + (2+\alpha)g_{31}\right], \tag{4.1}$$

where V is the open-circuit voltage of the cylinder, g_{33} and g_{31} are piezoelectric voltage constants (the 3-axis being the poling axis), and $\alpha \equiv (a/b)$. The sensitivity can be expressed in decibels using the expression

$$M = 20 \log\left(\frac{V}{P_0}\right). \tag{4.2}$$

The equations for the uncertainties in the sensitivities, δM and $\delta(V/P_0)$, are given in Appendix (A.1).

The sensitivity and its uncertainty are calculated for the BM024 ceramic cylinder using Eqs. (4.1), (4.2), (A.1), and (A.2). The known dimensions and piezoelectric constants, complete with typical manufacturing uncertainties, are

$$\begin{aligned} a \pm \delta a &= 9.5 \pm 0.1 \text{ mm} \\ b \pm \delta b &= 12.7 \pm 0.1 \text{ mm} \\ g_{33} \pm \delta g_{33} &= (25 \pm 1) \times 10^{-3} \text{ Vm/N} \\ g_{31} \pm \delta g_{31} &= -(11.5 \pm 0.6) \times 10^{-3} \text{ Vm/N}. \end{aligned} \tag{4.3}$$

Using these values, the theoretical free-field voltage sensitivity for the ceramic cylinder is

$$M \pm \delta M = -194.7 \pm 0.6 \text{ dB } re \text{ 1 V}/\mu\text{Pa}. \tag{4.4}$$

4.2 Sensitivity Correction

The measured free-field sensitivity of the BM024 hydrophone [-195 ± 1 dB from Section (3.1)], is an end-of-cable sensitivity and, as such, includes the parasitic capacitances associated with cables and hook-up wires, in addition to the capacitance of the ceramic cylinders at the electrodes. On the other hand, the sensitivity calculation in Section (4.1) does not include parasitic capacitances. We can, however, correct the theoretical sensitivity

given by Eq. (4.1), by multiplying it by the ratio of the capacitance between the ceramic electrodes, to the total end-of-cable capacitance [7]. This is expressed mathematically as

$$\left(\frac{V}{P_0}\right)_k = \left(\frac{C}{C+C_k}\right)\left(\frac{V}{P_0}\right) , \tag{4.5}$$

where $(V/P_0)_k$ is the reduced sensitivity at the end of the cable, C is the total capacitance at the electrodes of all ceramic cylinders, four in the case of the BM024 hydrophone, C_k is the total parasitic capacitance, and the sum $C+C_k$ is the end-of-cable capacitance. In decibels, the reduced sensitivity becomes

$$M_k = 20\log\left(\frac{V}{P_0}\right)_k . \tag{4.6}$$

We now estimate the correction factor in Eq. (4.5) by calculating the capacitance C in the numerator from theory, and then by estimating the sum $C+C_k$ in the denominator using the admittance measurements in Section (3.2).

The capacitance of one ceramic cylinder is given by the expression [8]

$$C_1 = \frac{2\pi\epsilon_0 k_{33}^{\mathrm{T}}\ell}{\ln(b/a)} , \tag{4.7}$$

where ϵ_0 is the permittivity of free space, k_{33}^{T} is the free, relative dielectric constant, and ℓ is the length of the cylinder. Therefore, the total capacitance of the four cylinders in the BM024 hydrophone is

$$C = 4C_1 , \tag{4.8}$$

since the cylinders are connected in parallel electrically.

The end-of-cable capacitance can be determined from Fig. 4 using

$$C + C_k = \frac{B}{2\pi f} , \tag{4.9}$$

where B is the measured susceptance at the frequency f. The expressions for the uncertainties in the corrected sensitivity equations above, are given in Appendix (A.2).

The reduced sensitivity of the BM024 hydrophone is calculated using the data in Eq. (4.3), in addition to the following known quantities;

$$\begin{aligned} \ell \pm \delta\ell &= 12.7 \pm 0.3 \text{ mm} \\ k_{33}^{\mathrm{T}} \pm \delta k_{33}^{\mathrm{T}} &= 1800 \pm 100 \\ B \pm \delta B &= 236 \pm 5 \ \mu\text{S} \\ f \pm \delta f &= 2000 \pm 5 \text{ Hz} . \end{aligned} \tag{4.10}$$

The error in the length of the cylinder, $\delta\ell$, is a typical manufacturing tolerance. Likewise, the error in the relative dielectric constant, $\delta k_{33}^{\mathrm{T}}$, is reasonable. The last two errors, δB and δf, are achievable with modern FFT analysers like the HP 3562A Dynamic Signal Analyser, used at the DREA calibration tank to measure the electrical admittance in Fig. 4. The magnitude of B is the measured value at 2 kHz.

Substituting these quantities into Eqs. (4.1), (4.5) to (4.9), and (A.2) to (A.6), we obtain the end-of-cable free-field voltage sensitivity

$$M_k \pm \delta M_k = -195.3 \pm 0.9 \text{ dB } re \text{ 1 V}/\mu\text{Pa}, \tag{4.11}$$

which agrees, within the stated uncertainty, with the measured sensitivity of -195 ± 1 dB *re* 1 V/μPa in Section (3.1).

The values of ceramic and end-of-cable capacitances, which were evaluated in the calculation of M_k, are

$$C \pm \delta C = 18 \pm 1 \text{ nF} \tag{4.12}$$

$$(C + C_k) \pm \delta(C + C_k) = 18.8 \pm 0.4 \text{ nF}, \tag{4.13}$$

respectively. The difference between these two capacitances is the total parasitic capacitance

$$C_k \pm \delta C_k = 1 \pm 1 \text{ nF}, \tag{4.14}$$

where the relatively large error is a direct result of the magnitude of the errors associated with the known input quantities, particularly $\delta k_{33}^{\mathrm{T}}$.

The calculation of the total parasitic capacitance is a semi-empirical one involving the difference between the theoretical capacitance of the cylindrical elements [Eq. (4.8)] and the measured end-of-cable capacitance of the hydrophone [Eq. (4.9)]. We can verify that the magnitude of C_k, so determined, is reasonable, by estimating the cable capacitance from the manufacturer's specifications [9], and calling this value the minimum parasitic capacitance (since it does not include parasitic capacitances inside the hydrophone assembly). Thus, at 101 pF/m, the 3.9 m Belden 8259 cable has a capacitance of 0.4 nF, which supports the result given by Eq. (4.14).

4.3 Resonance Frequencies

Within the frequency range 0 to 50 kHz there are four modes of resonance for the BM024 hydrophone. The in-air electrical admittance has been measured for each of these modes and the measured resonance frequencies are compared to theory.

4.3.1 Spurious Resonances

Two resonances, shown in the in-air electrical conductance of Fig. 7, occur at 3.20 ± 0.01 kHz and 3.40 ± 0.01 kHz. These peaks manifest themselves as significant perturbations to the otherwise constant sensitivity in Fig. 3.

As mentioned in Section (3.1) in connection with the sensitivity, the conductance peaks near 3.2 kHz are, in all likelihood, spurious resonances. Support for this conclusion is found in the small magnitudes of the conductance peaks, relative to the other resonances for the hydrophone. Probable causes of these resonances include nonuniform polarization in the piezoceramic cylinders, dimensional nonuniformities in the individual cylindrical elements, misalignment in the cylindrical assembly, and inhomogeneities in the polyurethane boot.

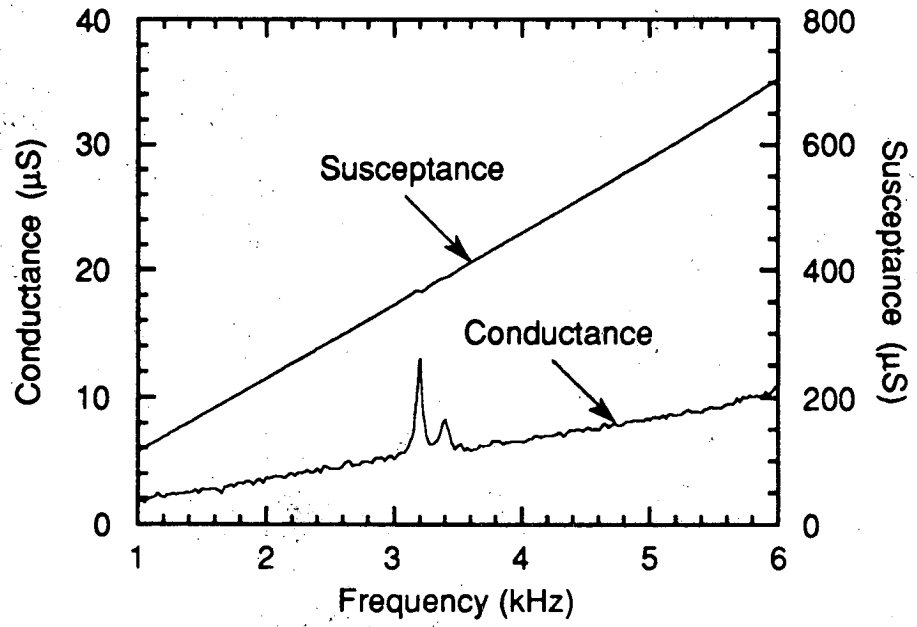

Figure 7: In-air electrical admittance of the BM024 hydrophone over the frequency range 1 to 6 kHz.

4.3.2 Flexural Resonance

The next resonance peak, as shown in Fig. 8, appears at 7.68 ± 0.01 kHz. This resonance occurs well below the frequency of the circumferential-mode resonance of the cylinder and limits the useful bandwidth. This resonance could be caused by a flexural mode, due to the segmented construction of the ceramic stack.

An approximate expression for the resonance frequencies of a flexural piezoelectric ceramic bar (bimorph or multimorph) is given in Ref. [10] for a cantilever bar with rectangular cross-section. The following modifications are made for the BM024 hydrophone: (i) the radius of gyration for a bar with rectangular cross-section is replaced by the radius of gyration for a bar with circular cross-section [11, 12], and (ii) the ceramic compliance, s_{11}^{E}, is replaced by an effective compliance for a bilaminar bar, s_b [2]. The result is

$$f_f = \frac{\pi D}{32L^2 \left(\rho s_b\right)^{\frac{1}{2}}} (1.194)^2 \,, \tag{4.15}$$

where D is the diameter and L is the effective length of the hydrophone assembly. The factor 1.194 is the lowest root of the transcendental equation

$$\cosh(kL)\cos(kL) = -1 \,, \tag{4.16}$$

where k is the wavenumber. The effective elastic compliance, s_b, is given by

$$s_b = \frac{4\epsilon_0 k_{33}^{\mathrm{T}} s_{11}^{\mathrm{D}} s_{11}^{\mathrm{E}}}{4\epsilon_0 k_{33}^{\mathrm{T}} s_{11}^{\mathrm{E}} - 3d_{31}^2} \,, \tag{4.17}$$

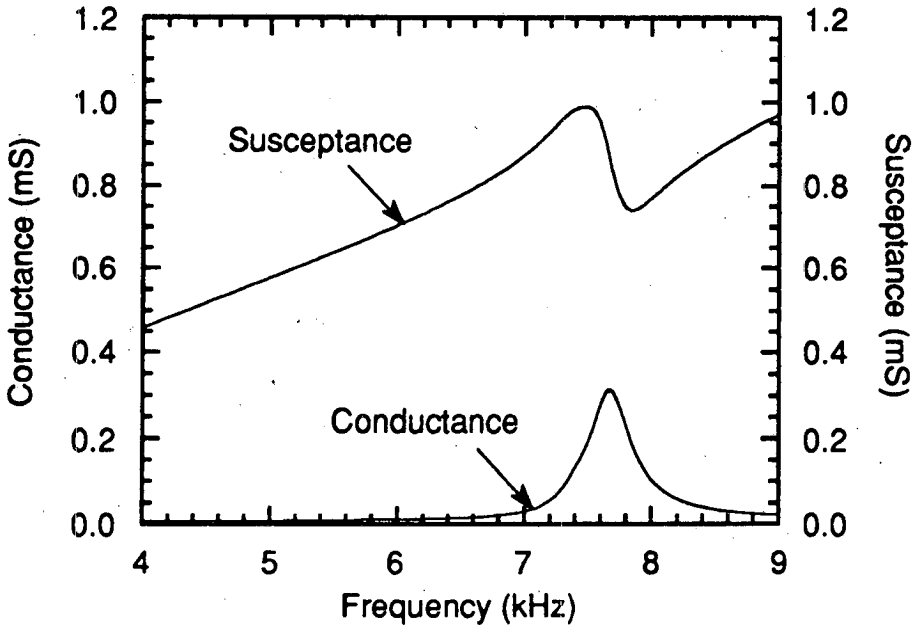

Figure 8: In-air electrical admittance of the BM024 hydrophone over the frequency range 4 to 9 kHz.

where s_{11}^{D} is the elastic compliance at constant charge density and d_{31} is the piezoelectric charge constant. The elastic compliances at constant charge density and constant electric field are related in the following way:

$$s_{11}^{\mathrm{D}} = s_{11}^{\mathrm{E}} - \frac{d_{31}^2}{\epsilon_0 k_{33}^{\mathrm{T}}} \,. \tag{4.18}$$

The expressions for the uncertainties in the flexural resonance frequency equations above are given in Appendix (B.1).

Using the following hydrophone dimensions and BM500 ceramic material constants

$$\begin{aligned} D \pm \delta D &= 31.64 \pm 0.07 \text{ mm} \\ L \pm \delta L &= 5.0 \pm 0.5 \text{ cm} \\ \rho \pm \delta\rho &= 7650 \pm 80 \text{ kg/m}^3 \\ s_{11}^{\mathrm{E}} \pm \delta s_{11}^{\mathrm{E}} &= (15.5 \pm 0.3) \times 10^{-12} \text{ m}^2/\text{N} \\ k_{33}^{\mathrm{T}} \pm \delta k_{33}^{\mathrm{T}} &= 1800 \pm 100 \\ d_{31} \pm \delta d_{31} &= -(160 \pm 8) \times 10^{-12} \text{ C/N} \,, \end{aligned} \tag{4.19}$$

we obtain the constants

$$\begin{aligned} s_{11}^{\mathrm{D}} \pm \delta s_{11}^{\mathrm{D}} &= (13.9 \pm 0.4) \times 10^{-12} \text{ m}^2/\text{N} \\ s_b \pm \delta s_b &= (15.1 \pm 0.4) \times 10^{-12} \text{ m}^2/\text{N} \,, \end{aligned} \tag{4.20}$$

and subsequently the flexural resonance frequency

$$f_f^- \pm \delta f_f^- \; = \; 5 \pm 1 \text{ kHz} \, . \tag{4.21}$$

The large error in f_f^- is due to the large uncertainty in the effective length L of the cantilever. The superscript on f_f^- is explained below. The compliance, s_b, lies between the compliances, s_{11}^{D} and s_{11}^{E}; it is 8% larger than the former and 3% smaller than the latter constant.

Note that we have used the properties of the ceramic cylinder, ρ and s_b, together with the diameter of the hydrophone assembly, D, instead of the smaller outside diameter of the ceramic cylinders, $2b$, in the calculations above. It would be more consistent to use an effective hydrophone assembly density and compliance since the cantilever has a cross-section that includes a tension bolt, an air gap, a ceramic cylinder, a polyurethane boot, and, depending on where the cross-section is taken, a brass end cap and ceramic washers.

An estimate of the effective density and compliance for the hydrophone can be made using the mechanics of materials method of summing the weighted properties (weighted by volume fraction) of each material in the cross-section. Hence, the effective density and compliance are approximately 3000 kg/m^3 and 40×10^{-12} m^2/N, respectively. The square root of the product of these properties is 3.5×10^{-4} s/m. The same quantity for BM500 ceramic, i.e. $(\rho s_b)^{\frac{1}{2}}$ in Eq. (4.15), is 3.4×10^{-4} s/m. Therefore, since these two factors are almost equal, Eq. (4.21) remains unchanged regardless of which set of properties are used.

Cantilever action requires a rigid boundary condition at one end of a flexible bar. The calculations above implicitly assume that the brass fittings on the cable end of the BM024 hydrophone are sufficiently massive to mechanically clamp one end. However, this is most likely not the case, and the hydrophone vibrates in flexure with end conditions intermediate between clamped-free and free-free. Since the calculations above were for a clamped-free bar vibrating in flexure, it is a lower bound, hence the minus sign superscript in Eq. (4.21). We now calculate the flexural resonance frequency of the hydrophone with two free ends and use this value as an upper bound.

Kinsler et al. [12] give the lowest flexural resonance frequency of a bar with free ends as

$$f_f = \frac{\pi D}{32 L^2 \left(\rho s_b\right)^{\frac{1}{2}}} (3.0112)^2 \, , \tag{4.22}$$

where the factor 3.0112 is the lowest root of the transcendental equation

$$\cosh(kL)\cos(kL) = 1 \, . \tag{4.23}$$

As before, the error equations are given in Appendix (B.1). Using the values of Eq. (4.19), together with

$$L \pm \delta L \; = \; 8.0 \pm 0.5 \text{ cm} \, , \tag{4.24}$$

which accounts for the added length of the vibrating brass fittings, the upper bound on the flexural resonance frequency is

$$f_f^+ \pm \delta f_f^+ \; = \; 13 \pm 2 \text{ kHz} \, . \tag{4.25}$$

The measured resonance frequency 7.68 ± 0.01 kHz lies between the upper and lower bounds given by Eqs. (4.25) and (4.21). Thus the most probable mode of vibration for this resonance is a flexural mode corresponding to a bar of circular cross-section with ends neither rigidly fixed nor completely free.

The derivation of the flexural frequencies above, assumes that the hydrophone diameter, D, is less than half its length, $L/2$. This geometry is sufficient to uncouple the flexural modes from other transverse modes. In the case of the free-free boundary conditions, this condition is satisfied, but it is not for the cantilever. However, the next resonance occurs at more than twice the flexural frequency, and according to Martin [13], the flexural frequency is reduced by less than 1% due to mode coupling. This error is much smaller than that in Eq. (4.21) and can therefore be ignored.

4.3.3 Longitudinal Resonance

The next resonance occurs at 16.94 ± 0.01 kHz, as shown in Fig. 9. This mode also occurs below the circumferential mode of the cylinder, and could possibly be a longitudinal stack mode.

The fundamental resonance frequency for an unloaded, lossless bar of uniform cross-section, with both ends free, is given by [12, 14] as

$$f_\ell = \frac{1}{2L\,(\rho s_b)^{\frac{1}{2}}} \,. \tag{4.26}$$

If the bar is fixed at one end and free at the other, then the fundamental resonance frequency is $f_\ell/2$ [12]. Just as we did for the flexural resonance, we let these two frequencies be the upper and lower bounds, f_ℓ^+ and f_ℓ^- respectively, for the longitudinal resonance frequency.

Again, using the values in Eq. (4.19) and the length in Eq. (4.24), we obtain the following bounds

$$f_\ell^+ \pm \delta f_\ell^+ \;=\; 18 \pm 1 \text{ kHz} \,, \tag{4.27}$$

$$f_\ell^- \pm \delta f_\ell^- \;=\; 9.2 \pm 0.6 \text{ kHz} \,, \tag{4.28}$$

where the errors are given by the expression in Appendix (B.2).

The measured resonance frequency lies within the two bounds given by Eqs. (4.27) and (4.28) and, therefore, is most likely a longitudinal mode.

4.3.4 Circumferential Resonance

Finally, the measured circumferential mode frequency of the ceramic cylinder is 41.45 ± 0.02 kHz, as shown in Fig. 10. This value is verified using the equations derived by Haskins and Walsh [15] for the resonances of a radially polarized, ferroelectric cylindrical tube. Assuming that the surfaces are stress-free and that the wall thickness is small, the resonance frequencies are given by

$$\left(\frac{f}{f_r}\right)^4 \left[1 - (\sigma_{12}^{\mathrm{E}})^2\right] - \left(\frac{f}{f_r}\right)^2 \left[1 + (n\pi\bar{a}/\ell)^2\right] + (n\pi\bar{a}/\ell)^2 = 0 \,, \tag{4.29}$$

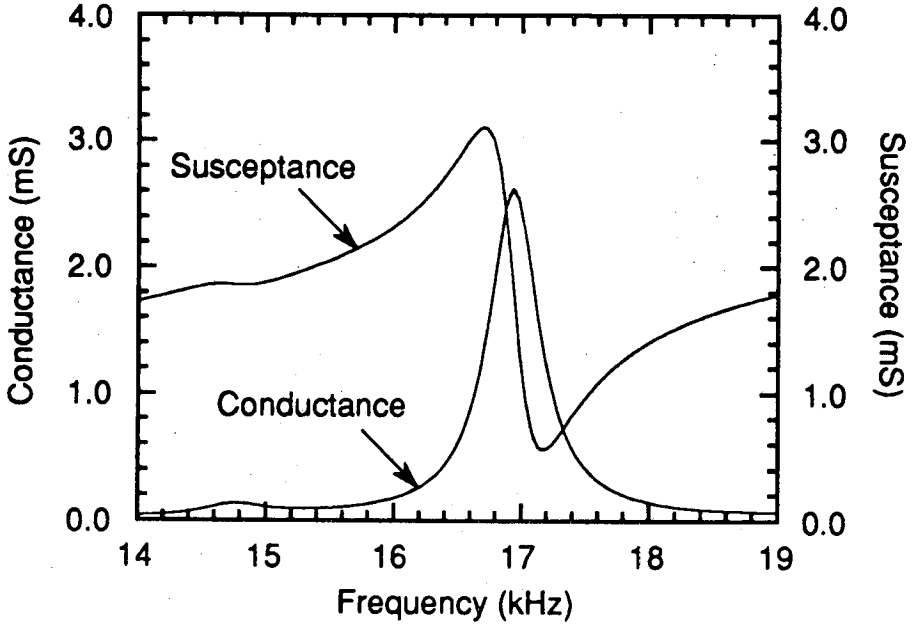

Figure 9: In-air electrical admittance of the BM024 hydrophone over the frequency range 14 to 19 kHz.

which is quadratic in $(f/f_r)^2$. End effects have been neglected.

In Eq. (4.29), the mean radius of the cylinder is $\bar{a}$, the longitudinal nodal number is $n = 1, 3, 5, \ldots$, f_r is the ring resonance, given by [14]

$$f_r = \frac{1}{2\pi\bar{a}\,(\rho s_{11}^{\mathrm{E}})^{\frac{1}{2}}}\,, \tag{4.30}$$

and σ_{12}^{E} is the Poisson's ratio at constant electric field, defined by

$$\sigma_{12}^{\mathrm{E}} = -\frac{s_{12}^{\mathrm{E}}}{s_{11}^{\mathrm{E}}}\,, \tag{4.31}$$

where s_{11}^{E} and s_{12}^{E} are elastic compliances at constant electric field.

Solving Eq. (4.29) for $n = 1$, we obtain the following expression for the lowest circumferential resonance frequency:

$$f_c = f_r \left[\frac{1 + (\pi\bar{a}/\ell)^2 - \{[1 + (\pi\bar{a}/\ell)^2]^2 - 4(\pi\bar{a}/\ell)^2[1 - (\sigma_{12}^{\mathrm{E}})^2]\}^{\frac{1}{2}}}{2[1 - (\sigma_{12}^{\mathrm{E}})^2]}\right]^{\frac{1}{2}}\,. \tag{4.32}$$

The expressions for the uncertainties in the circumferential resonance frequency equations above are given in Appendix (B.3).

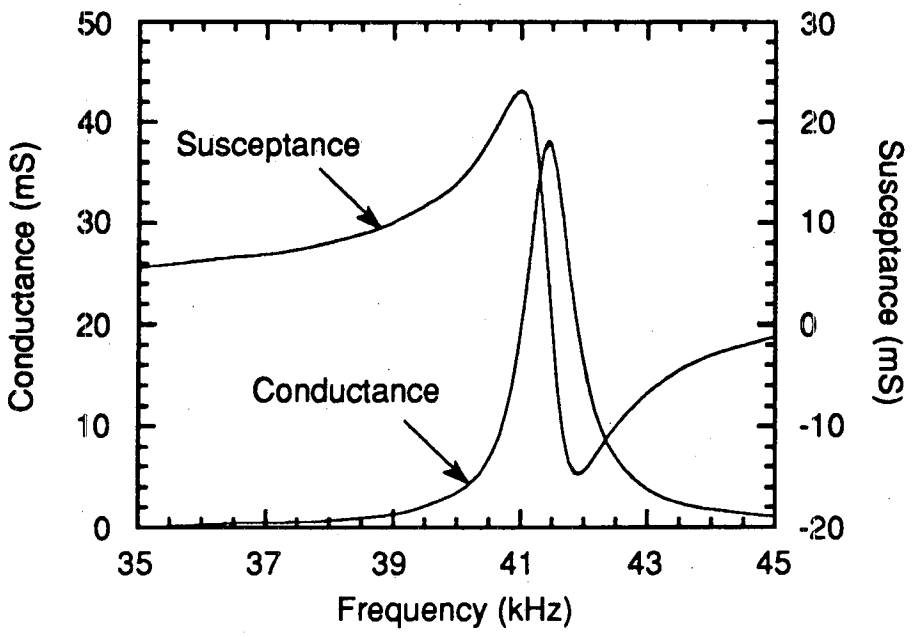

Figure 10: In-air electrical admittance of the BM024 hydrophone over the frequency range 35 to 45 kHz.

The following quantities for the BM500 ceramic cylinders are used to evaluate the circumferential resonance and its error;

$$\begin{aligned} \ell \pm \delta\ell &= 12.7 \pm 0.3 \text{ mm} \\ \bar{a} \pm \delta\bar{a} &= 11.1 \pm 0.1 \text{ mm} \\ \rho \pm \delta\rho &= 7650 \pm 80 \text{ kg/m}^3 \\ s_{11}^{\mathrm{E}} \pm \delta s_{11}^{\mathrm{E}} &= (15.5 \pm 0.3) \times 10^{-12} \text{ m}^2/\text{N} \\ \sigma_{12}^{\mathrm{E}} \pm \delta\sigma_{12}^{\mathrm{E}} &= 0.31 \pm 0.03 \,, \end{aligned} \tag{4.33}$$

where the mean radius, $\bar{a}$, is the average of a and b in Eq. (4.3). The resulting resonance frequency is

$$f_c \pm \delta f_c = 41.1 \pm 0.6 \text{ kHz} \,, \tag{4.34}$$

which agrees with the measured value, within the stated error limits.

5 Conclusions

The performance of an end-capped cylindrical hydrophone, manufactured by B.M. Hi-Tech Division of Sensor Technology Limited, has been investigated. The useful frequency bandwidth extends up to 5 kHz, and the measured value of the free-field voltage sensitivity in this band is -195 dB *re* 1 V/μPa, which agrees with the well-established sensitivity theory of Langevin. Three resonance frequencies have been measured and attributed to flexural (7.68 kHz), longitudinal (16.94 kHz), and circumferential (41.45 kHz) modes of vibration. Since the flexural resonance is the lowest in frequency, it limits the useful bandwidth. It may be possible to extend the useful bandwidth to frequencies higher than 5 kHz by (a) reducing the number of elements in the stack, thereby reducing the likelihood of exciting flexural modes, and (b) reducing the overall length of the hydrophone, which would move the longitudinal resonance to higher frequencies. Finally, the spurious resonances observed at 3.2 and 3.4 kHz may be suppressed by ensuring that the ceramic elements are uniform in their dimensions and properties, by reducing the void content of the polyurethane boot, and by carefully aligning the various hydrophone components. Of course, the implementation of these improvements may increase the expense of manufacturing this "low-cost" hydrophone design.

References

[1] J.M. Powers, "Long range hydrophones," in *The Applications of Ferroelectric Polymers*, edited by T.T. Wang, J.M. Herbert, and A.M. Glass (Chapman and Hall, New York, 1988).

[2] R.S. Woollett, *The Flexural Bar Transducer*, (Naval Underwater Systems Center, Newport, RI, 1986).

[3] A.C. Tims, "A new capped-cylinder design for an underwater sound transducer (USRD Type F50)," J. Acoust. Soc. Am. **51**, 1751-1758 (1972).

[4] R.J. Bobber, *Underwater Electroacoustic Measurements* (Naval Research Laboratory, Washington, D.C., 1970).

[5] J.E. Blue, "Evaluation of precision and accuracy in the calibration of hydrophones," NRL Report 7571, Naval Research Laboratory, March 1973.

[6] R.A. Langevin, "The electro-acoustic sensitivity of cylindrical ceramic tubes," J. Acoust. Soc. Am. **26**, 421-427 (1954).

[7] H.A.J. Rijnja, "Small sensitive hydrophones," Acustica **27**, 182-188 (1972).

[8] S. Hanish, *A Treatise on Acoustic Transducers, Volume II, Acoustic Transducers* (Naval Research Laboratory, Washington, D.C., 1983).

[9] *Master Catalog* (Belden Wire and Cable, Richmond, IN, 1989), p. 127.

[10] *Piezoelectric Ceramics*, edited by J. van Randeraat (N.V. Philips' Gloeilampenfabrieken, Eindhoven, Netherlands, 1968).

[11] P.M. Morse, *Vibration and Sound* (American Institute of Physics, New York, 1986).

[12] L.E. Kinsler, A.R. Frey, A.B. Coppens, and J.V. Sanders, *Fundamentals of Acoustics* (Wiley, New York, 1982), 3rd edition.

[13] G.E. Martin, "Vibrations of longitudinally polarized ferroelectric cylindrical tubes," J. Acoust. Soc. Am. **510**, 510-520 (1963).

[14] D.A. Berlincourt, D.R. Curran, and H. Jaffe, "Piezoelectric and Piezomagnetic materials and their function in transducers," in *Physical Acoustics*, Volume I, Part A, edited by W.P. Mason (Academic Press, New York, 1964).

[15] J.F. Haskins and J.L. Walsh, "Vibrations of ferroelectric cylindrical shells with transverse isotropy. I. Radially polarized case," J. Acoust. Soc. Am. **29**, 729-734 (1957).

[16] J.R. Taylor, *An Introduction to Error Analysis* (University Science Books, Mill Valley, CA, 1982).

Appendix A

The uncertainty in all of the calculated quantities in this paper are evaluated using the propagation of error techniques found in Taylor [16]. The basic assumptions underlying these techniques are that the measured errors are independent and random. The equations for the uncertainties in the sensitivity calculations are summarized below.

A.1 Errors in the Free-Field Sensitivity Calculations

Given the errors δg_{33}, δg_{31}, δa, and δb, then the uncertainty in the free-field sensitivity is given by

$$\delta M = 20\log(e)\left(\frac{V}{P_0}\right)^{-1}\delta\left(\frac{V}{P_0}\right), \tag{A.1}$$

where e is the base of the natural logarithms, and the uncertainty in (V/P_0) is

$$\delta\left(\frac{V}{P_0}\right) = \left\{\frac{b^2(1-\alpha)^2}{(1+\alpha)^2}(\delta g_{33})^2 + \frac{b^2(2+\alpha)^2}{(1+\alpha)^2}(\delta g_{31})^2 + \frac{(2g_{33}+g_{31})^2}{(1+\alpha)^4}(\delta a)^2 + \frac{[(1+2\alpha-\alpha^2)g_{33}+(2+4\alpha+\alpha^2)g_{31}]^2}{(1+\alpha)^4}(\delta b)^2\right\}^{\frac{1}{2}}. \tag{A.2}$$

A.2 Errors in the Corrected Sensitivity Calculations

The errors required to calculate the corrected sensitivity are determined by the following expressions:

$$\delta M_k = 20\log(e)\left(\frac{V}{P_0}\right)_k^{-1}\delta\left(\frac{V}{P_0}\right)_k, \tag{A.3}$$

$$\delta\left(\frac{V}{P_0}\right)_k = \left(\frac{V}{P_0}\right)_k\left\{\left[\frac{\delta(V/P_0)}{(V/P_0)}\right]^2 + \left[\frac{\delta C}{C}\right]^2 + \left[\frac{\delta(C+C_k)}{C+C_k}\right]^2\right\}^{\frac{1}{2}}, \tag{A.4}$$

$$\delta C = C\left\{\frac{(\delta\ell)^2}{\ell^2} + \frac{(\delta k_{33}^{\mathrm{T}})^2}{(k_{33}^{\mathrm{T}})^2} + \frac{(\delta b)^2}{[b\ln(b/a)]^2} + \frac{(\delta a)^2}{[a\ln(b/a)]^2}\right\}^{\frac{1}{2}}, \tag{A.5}$$

and

$$\delta(C+C_k) = (C+C_k)\left\{\left[\frac{\delta B}{B}\right]^2 + \left[\frac{\delta f}{f}\right]^2\right\}^{\frac{1}{2}}, \tag{A.6}$$

where the errors δC and $\delta(C+C_k)$ are calculated from the known errors δa, δb, $\delta\ell$, $\delta k_{33}^{\mathrm{T}}$, δB, and δf. The error $\delta(V/P_0)$ is given by Eq. (A.2).

Appendix B

The equations for the uncertainties in the flexural, longitudinal, and circumferential resonance frequencies are summarized below.

B.1 Errors in the Flexural Resonance

The errors for the equations used to calculate the upper and lower bounds on the flexural resonance frequency are given by

$$\delta s_{11}^{\mathrm{D}} = \frac{\left\{[\epsilon_0 (k_{33}^{\mathrm{T}})^2]^2 (\delta s_{11}^{\mathrm{E}})^2 + (2k_{33}^{\mathrm{T}} d_{31})^2 (\delta d_{31})^2 + d_{31}^4 (\delta k_{33}^{\mathrm{T}})^2\right\}^{\frac{1}{2}}}{\epsilon_0 (k_{33}^{\mathrm{T}})^2}, \tag{B.7}$$

$$\delta s_b = \frac{s_b}{s_{11}^{\mathrm{D}}} \left[(\delta s_{11}^{\mathrm{D}})^2 + \left(\frac{s_{11}^{\mathrm{D}} - s_b}{s_{11}^{\mathrm{E}}} \right)^2 (\delta s_{11}^{\mathrm{E}})^2 + \left(\frac{s_{11}^{\mathrm{D}} - s_b}{k_{33}^{\mathrm{T}}} \right)^2 (\delta k_{33}^{\mathrm{T}})^2 + \left(\frac{3 s_b d_{31}}{2\epsilon_0 k_{33}^{\mathrm{T}} s_{11}^{\mathrm{E}}} \right)^2 (\delta d_{31})^2 \right]^{\frac{1}{2}}, \tag{B.8}$$

and

$$\delta f_f = f_f \left[\left(\frac{\delta D}{D} \right)^2 + 4 \left(\frac{\delta L}{L} \right)^2 + \left(\frac{\delta \rho}{2\rho} \right)^2 + \left(\frac{\delta s_b}{2 s_b} \right)^2 \right]^{\frac{1}{2}}, \tag{B.9}$$

where the errors δD, δL, $\delta \rho$, $\delta s_{11}^{\mathrm{E}}$, $\delta k_{33}^{\mathrm{T}}$, and δd_{31} are known.

B.2 Errors in the Longitudinal Resonance

The errors in the upper and lower frequency bounds for the longitudinal resonance frequency are given by

$$\delta f_\ell = f_\ell \left[\left(\frac{\delta L}{L} \right)^2 + \left(\frac{\delta \rho}{2\rho} \right)^2 + \left(\frac{\delta s_b}{2 s_b} \right)^2 \right]^{\frac{1}{2}}. \tag{B.10}$$

B.3 Errors in the Circumferential Resonance

The error in the circumferential resonance frequency is determined by making the following three definitions,

$$\zeta = 1 - (\sigma_{12}^{\mathrm{E}})^2, \tag{B.11}$$

$$\xi = (\pi \bar{a}/\ell)^2, \tag{B.12}$$

$$\beta = \{1 + \xi - [(1+\xi)^2 - 4\zeta\xi]^{\frac{1}{2}}\}^{\frac{1}{2}}, \tag{B.13}$$

and writing the errors as

$$\delta f_c = \frac{1}{2(2\zeta)^{\frac{1}{2}}} \left\{ (2\beta)^2 (\delta f_r)^2 + \left[\frac{2\pi^2 \bar{a} f_r (2\zeta - \beta^2)}{\beta \ell^2 (1 + \xi - \beta^2)} \right]^2 (\delta \bar{a})^2 \right.$$
$$+ \left[\frac{2\sigma_{12}^{\mathrm{E}} f_r [2\zeta\xi - \beta^2(1 + \xi - \beta^2)]}{\beta\zeta(1 + \xi - \beta^2)} \right]^2 (\delta\sigma_{12}^{\mathrm{E}})^2 \qquad \text{(B.14)}$$
$$\left. + \left[\frac{2\pi^2 \bar{a}^2 f_r (2\zeta - \beta^2)}{\beta \ell^3 (1 + \xi - \beta^2)} \right]^2 (\delta\ell)^2 \right\}^{\frac{1}{2}},$$

where δf_r is given by the expression

$$\delta f_r = \left[\frac{(2\rho s_{11}^{\mathrm{E}})^2 (\delta\bar{a})^2 + (\bar{a} s_{11}^{\mathrm{E}})^2 (\delta\rho)^2 + (\bar{a}\rho)^2 (\delta\sigma_{11}^{\mathrm{E}})^2}{16\pi^2 \bar{a}^4 \rho^3 (\sigma_{11}^{\mathrm{E}})^3} \right]^{\frac{1}{2}}. \qquad \text{(B.15)}$$

DOCUMENT CONTROL DATA

(Security classification of title, body of abstract and indexing annotation must be entered when the overall document is classified)

1. ORIGINATOR (The name and address of the organization preparing the document. Organizations for whom the document was prepared, e.g. Establishment sponsoring a contractor's report, or tasking agency, are entered in section 8.)

Defence Research Establishment Atlantic
P.O. Box 1012, Dartmouth, N.S. B2Y 3Z7

2. SECURITY CLASSIFICATION (Overall security of the document including special warning terms if applicable.)

Unclassified

3. TITLE (The complete document title as indicated on the title page. Its classification should be indicated by the appropriate abbreviation (S,C,R or U) in parentheses after the title.)

An End-Capped Cylindrical Hydrophone for Underwater Sound Detection

4. AUTHORS (Last name, first name, middle initial. If military, show rank, e.g. Doe, Maj. John E.)

Jones, D.F., Prasad, S.E., Kavanaugh, S.R.

5. DATE OF PUBLICATION (Month and year of publication of document.)

June 1992

6a. NO. OF PAGES (Total containing information. Include Annexes, Appendices, etc.)

28

6b. NO. OF REFS. (Total cited in document.)

16

6. DESCRIPTIVE NOTES (The category of the document, e.g. technical report, technical note or memorandum. If appropriate, enter the type of report, e.g. interim, progress, summary, annual or final. Give the inclusive dates when a specific reporting period is covered.)

Technical Memorandum

8. SPONSORING ACTIVITY (The name of the department project office or laboratory sponsoring the reseach and development. include the address.)

Defence Research Establishment Atlantic
P.O. Box 1012, Dartmouth, N.S. B2Y 3Z7

9a. PROJECT OR GRANT NUMBER (If appropriate, the applicable research and development project or grant number under which the document was written. Please specify whether project or grant.)

DRDM 03

9b. CONTRACT NUMBER (If appropriate, the applicable number under which the document was written.)

10a. ORIGINATOR'S DOCUMENT NUMBER (The official document number by which the document is identified by the originating activity. This number mrst be unique to this document.)

DREA Technical Memorandum 92/216

10b. OTHER DOCUMENT NUMBERS (Any other numbers which may be assigned this document either by the originator or by the sponsor.)

11. DOCUMENT AVAILABILITY (Any limitations on further dissemination of the document, other than those imposed by security classification)

- (X) Unlimited distribution
- ( ) Distribution limited to defence departments and defence contractors; further distribution only as approved
- ( ) Distribution limited to defence departments and Canadian defence contractors; further distribution only as approved
- ( ) Distribution limited to government departments and agencies; futher distribution only as approved
- ( ) Distribution limited to defence departments; further distribution only as approved
- ( ) Other (please specify):

12. DOCUMENT ANNOUNCEMENT (Any limitation to the bibliographic annoucement of this document. This will normally correspond to the Document Availability (11). However, where futher distribution (beyond the audience specified in 11) is possible, a wider announcement audience may be selected.)

Unlimited

13. ABSTRACT (a brief and factual summary of the document. It may also appear elsewhere in the body of the document itself. It is highly desirable that the abstract of classified documents be unclassified. Each paragraph of the abstract shall begin with an indication of the security classification of the information in the paragraph (unless the document itself is unclassified) represented as (S), (C), (R), or (U). It is not necessary to include here abstracts in both offical languages unless the text is bilingual).

A small end-capped cylindrical hydrophone has been designed and built for use as a low cost, general purpose hydrophone in the frequency range 15 Hz to 5 kHz. The measured free-field voltage sensitivity of the hydrophone is -195 dB re 1 V/uPa, which agrees with the theoretical sensitivity for capped piezoelectric ceramic tubes. In addition, three resonance frequencies below 45 kHz have been measured and identified with circumferential, longitudinal, and flexural modes of vibration.

14. KEYWORDS, DESCRIPTORS or IDENTIFIERS (technically meaningful terms or short phrases that characterize a document and could be helpful in cataloguing the document. They should be selected so that no security classification is required. Identifiers, such as equipment model designation, trade name, military project code name, geographic location may also be included. If possible keywords should be selected from a published thesaurus, e.g. Thesaurus of Engineering and Scientific Terms (TEST) and that thesaurus-identified. If it is not possible to select indexing terms which are Unclassified, the classification of each should be indicated as with the title.)

sonar transducers
hydrophones
acoustic calibration
sensors